

ARTICLE OPEN



Autism spectrum disorder common variants associated with regional lobe volume variations at birth: cross-sectional study in 273 European term neonates in developing human connectome project

Hai Le ¹✉, Daphna Fenchel¹, Konstantina Dimitrakopoulou², Hamel Patel ³, Charles Curtis^{3,4}, Lucilio Cordero-Grande ^{1,5}, A. David Edwards ¹, Joseph Hajnal ¹, Jacques-Donald Tournier¹, Maria Deprez¹ and Harriet Cullen ^{1,6}

© The Author(s) 2025

Increasing lines of evidence suggest cerebral overgrowth in autism spectrum disorder (ASD) children in early life, but few studies have examined the effect of ASD common genetic variants on brain volumes in a general paediatric population. This study examined the association between ASD polygenic risk score (PRS) and volumes of the frontal, temporal, parietal, occipital, fronto-temporal and parieto-occipital lobes in 273 term-born infants of European ancestry in the developing Human Connectome Project. ASD PRS was positively associated with frontal ($\beta = 0.027$, $p_{FDR} = 0.04$) and fronto-temporal ($\beta = 0.024$, $p_{FDR} = 0.01$) volumes, but negatively with parietal ($\beta = -0.037$, $p_{FDR} = 0.04$) and parieto-occipital ($\beta = -0.033$, $p_{FDR} = 0.01$) volumes. This preliminary result suggests the potential involvement of ASD common genetic variants in early structural variations linked to ASD.

Translational Psychiatry (2025)15:41; <https://doi.org/10.1038/s41398-025-03253-2>

INTRODUCTION

Early neuroanatomical differences have been associated with autism spectrum disorder (ASD) [1], but the role of ASD common genetic variants on normal brain development in neonates remains unclear. Preliminary examination of additive effects of the single nucleotide polymorphisms (SNPs) as measured by polygenic risk scores (PRS) has suggested links between ASD polygenic risk and structural abnormalities in young children. Recently, in two general paediatric populations between 9–11 and 3–14 years of age, findings revealed associations between ASD PRS and regional cortical thickness [2] and gyrification [3]. Despite small effect sizes, these results demonstrate possible brain morphological alterations associated with ASD common genetic variants.

Increasing lines of evidence suggest early brain structural variations are likely to precede ASD diagnosis and can be detected in the first two years of life [4]. For instance, greater extra-axial cerebral spinal fluid [5], hyper-expansion of cortical surface area [1], and ventriculomegaly [6] can be found in infants with ASD or at high familial risk of the disease as early as six months after birth. Similarly, total brain tissue and regional lobe volumes appear larger in ASD cases between two to four years old as compared with controls [7–9]. Further evidence suggests these regional lobe

volume variations may not be consistent throughout the cerebrum and that frontal and temporal lobes are relatively more affected than parietal and occipital lobes [10–13]. Taken together, this points toward possible disruption to the normal neurodevelopmental process (i.e., from primary to more complex functions) in the disease [14].

Common genetic variants appear to explain at least 12% of the heritability of ASD [15]. Functional annotation of the genetic loci revealed enrichment in genes particularly important during fetal corticogenesis [15, 16]. Similarly, a recent transcriptomic analysis of postmortem ASD tissues spanning four cortical lobes found evidence of variable changes in genetic expression of ASD risk genes along the anterior-posterior axis [17] reflecting possible alterations to fundamental elements of cortical organisation in the disease. Concurrently, the neonatal brain is most rapidly changing immediately after birth [18, 19]. The first two postnatal years are characterised by dynamic, regionally non-uniform and protracted brain growth [18]. Disruption to normal development during this critical window as a result of either genetic or environmental factors may have long-lasting effects on brain structure and function [20].

Given the evidence of regional lobe volume variations associated with the disease and possible involvement of ASD risk

¹Research Department of Early Life Imaging, School of Biomedical Engineering and Imaging Sciences, King's College London, London, UK. ²Translational Bioinformatics Platform, NIHR Biomedical Research Centre, Guy's and St. Thomas' NHS Foundation Trust and King's College London, London, UK. ³NIHR BioResource Centre Maudsley, NIHR Maudsley Biomedical Research Centre at South London and Maudsley NHS Foundation Trust & Institute of Psychiatry, Psychology and Neuroscience, King's College London, London, UK. ⁴Social Genetic & Developmental Psychiatry Centre, Institute of Psychiatry, Psychology and Neuroscience, King's College London, London, UK. ⁵Biomedical Image Technologies, ETSI Telecomunicación, Universidad Politécnica de Madrid & CIBER-BBN, ISCIII, Madrid, Spain. ⁶Department of Medical and Molecular Genetics, School of Basic and Medical Biosciences, King's College London, London, UK. ✉email: L.haibg@gmail.com

Received: 5 October 2023 Revised: 11 December 2024 Accepted: 21 January 2025

Published online: 05 February 2025

genes in early neurodevelopmental process [15, 17], the current work aimed to examine the association between ASD common variants and regional lobe volumes in the general population at birth.

METHODS

Cohort

The data used were analysed from infants, who were recruited from St. Thomas' Hospital London, UK as part of the third release of developing Human Connectome Project (dHCP) (<https://biomedica.github.io/dHCP-release-notes/>) [21]. The inclusion criteria for imaging were live infants between 23 and 44 weeks of gestational age, estimated from the mother's last menstrual period and confirmed where possible by ultrasound. On the other hand, infants were excluded if they were not suitable for MRI (e.g., too unwell to tolerate the scanning period) or proper communication about the trial could not be conveyed to the parents (e.g., language difficulties). The dHCP was conducted according to the principles of the Declaration of Helsinki and ethical approval was given from the UK National Research Ethics Service. Written parental consent was provided for all subjects.

Genotyping and genetic quality control. The genetic data quality control and preprocessing steps used in this study are described in [22]. Briefly, of the 842 saliva samples, genotype data were collected (Oragene DNA OG-250 kit) and genotyped for SNPs genome-wide on the Illumina Infinium Omni5-4 v1.2 array. If multiple samples were provided, only one per individual was retained for analysis (randomly chosen). Excluded were also genotyped data based on the following criteria: completeness of less than 95%, gender discrepancy and genotyping failure of more than 1% of the SNPs. If the relatedness score between any individual pair was above a cut-off ($\pi_{\text{hat}} > 0.1875$), only one sample was randomly retained. Finally, SNPs were filtered based on the following criteria: being non-autosomal, having minor allele frequency less than 0.05, missing in more than 1% of individuals or deviating from Hardy-Weinberg equilibrium with a p -value $< 1 \times 10^{-5}$. This resulted in a sample of 754 individuals with high-quality genetic data encompassing 1 570 035 SNPs.

Data pre-processing

Given the strong effect of prematurity on the imaging phenotype, out of 887 available imaging scans, only those of term-born infants (born after at least 37 weeks of gestational age (GA)) were selected for analysis ($n = 582$ scans). Briefly, infants' brain scans were obtained during their natural sleep using a dedicated neonatal brain imaging system on a 3T Philips Achieva scanner [23]. The bespoke imaging system deposited infants in a standardized pose with adjustments only in the head-to-foot direction at the start of scanning. The field of view was set to accommodate 95% of late-term neonates. The scanning software was optimised to gradually ramp up gradient waveforms over 5 s before starting each sequence to prevent waking the infants. The full imaging protocol included the acquisition of calibration scans, anatomical images (T1w and T2w), resting-state functional and diffusion MRI at an average rate of 27 slices per second and a total scan duration of 1 h 3 min and 11 s. Specifically, T2-weighted MRI was acquired using a TSE sequence with parameters $TR = 12$ s, $TE = 156$ ms, and resolution (mm) $0.8 \times 0.8 \times 1.6$. A series of motion correction [24] and super-resolution reconstruction [25] techniques were then employed to produce images of resolution (mm) $0.5 \times 0.5 \times 0.5$. Subsequently, the T2 images were segmented with the DrawEM neonatal segmentation algorithm (<https://github.com/MIRTK/DrawEM>) [26]. This technique utilized spatial priors of 50 brain regions in the form of 20 manually segmented atlases [27] in combination with tissue segmentation using an Expectation-Maximisation technique to model intensities of different tissue classes and their subdivisions. This allowed the images to be accurately parcellated into 87 regions (Fig. 1A). The quality control was performed as a part of the dHCP minimal processing pipeline [28]. The absolute volumes of each structure were calculated as the total number of voxels multiplied by the voxel dimension [29]. Images with a radiology score of 5 (i.e., major brain lesions) denoted by clinical experts were excluded (26 scans removed). Finally, of the duplicate scans, the first imaging session was retained (2 scans removed).

Volumetric data. From the original 87 segmented regions, the cortical grey and white matter regions that made up the frontal, temporal, occipital

and parietal lobes were selected in accordance with previous studies [13, 30]. Here, the total grey and white matter volumes in both hemispheres of six brain regions – frontal, temporal, occipital, parietal, fronto-temporal and parieto-occipital were calculated. In addition, the brain volumes of the superior temporal gyrus (middle and posterior part), the inferior temporal gyri (anterior and posterior part) and the anterior temporal lobe (medial and lateral part) were summed up to designate the temporal lobe. The lateral occipitotemporal gyrus and gyrus fusiform (posterior and anterior part) were included in the volume of the occipital lobe (Fig. 1B). The total brain tissue volume (TBV) was computed as the sum of the volumes of cortical white and grey matter, deep grey matter, cerebellum and brainstem.

Populations stratification. Ancestry subpopulations were identified by merging our cohort of 754 infants with 2504 individuals from the 1000 Genomes Project [31] using a subset of common autosomal SNPs. Principal component analysis (PCA) was then performed on the resulting genetic dataset with PLINK and principal components (PCs) generated were plotted to visually assign individuals to ancestral subgroups. Since the discovery sample used in the genome-wide association study included exclusively Danish individuals, only infants of European ancestry were chosen for the ongoing analysis. Here, 429 (57%) infants were determined to have European ancestry.

European ancestry PCs were derived from the genetic data of the 429 infants using PCA, and a visual examination of the PC pairwise scatterplots was carried out to exclude European ancestral group outliers (6 individuals excluded). Finally, of the remaining infants of European ancestry, 273 were born at term and examined in this study (Table 1; Fig. 2).

Polygenic risk score. The summary statistics used to determine individual PRS were derived from the largest to date ASD GWAS [15]. This analysis was performed on 18 381 individuals with ASD and 27 969 controls from a unique Danish population [32]. PRS for each dHCP infant were estimated using PRSice-2 at 10 different p -value thresholds (P_T): 10^{-8} , 10^{-6} , 10^{-5} , 0.0001, 0.001, 0.01, 0.05, 0.1, 0.5, and 1, such that each score was composed of only those SNPs with ASD GWAS association p -value less than the respective threshold. Genotype data of European individuals in the 1000 Genomes project was used as the external linkage disequilibrium reference panel [31]. PCA was then carried out on all 10 raw PRS values to obtain the first principal component (PRS-PC1) [33]. In accordance with several genetic-neuroimaging studies, this unsupervised approach was selected due to its ease of implementation and reduction of multiple testing without loss of power [34–36]. In the present study, PRS-PC1 explained 44% of the total variance in PRS scores and was positively associated with PRS at all P_T (Supplementary Fig. 1).

Statistical analysis

For each of the 6 dependent variables of interest (frontal, temporal, occipital, parietal, fronto-temporal, parieto-occipital lobe volumes), a linear regression was performed with PRS-PC1 as the independent variable, and the first 3 European ancestry PC, GA, postmenstrual age at scan (PMA), sex and TBV as covariates (i.e., $\text{Volume} = \text{PRS-PC1} + \text{Ancestry} + \text{GA} + \text{PMA} + \text{Sex} + \text{TBV}$). Previous studies indicated PMA, GA and sex can account for differences in regional brain volumes in neonates [29, 37]. Ancestry PCs were included to account for genetic differences due to ancestry. TBV was included to account for the overall brain growth. The multiple-testing correction was carried out using the false discovery rate (FDR) method. Results with p -value $FDR < 0.05$ were considered statistically significant.

Given our relatively small cohort, the results were further examined using three additional stability tests. Firstly, the sample was randomly divided into 2 data sets. PCA of the PRS and subsequent regression analysis described above were carried out on both data sets separately, the results of which were then compared. Here, the result was considered consistent if both sets yielded associations reported in the primary analysis. This test was repeated 1000 times using different random splits. Secondly, the brain volume of the top and bottom 20% of the PRS distribution at each P_T was compared using t -tests. Thirdly, the regression analysis described above was performed with each of the 10 P_T instead of PRS-PC1.

Exploratory gene-set enrichment analysis

To further examine if ASD common genetic variants most associated with lobe volumes converged on relevant biological pathways, an exploratory

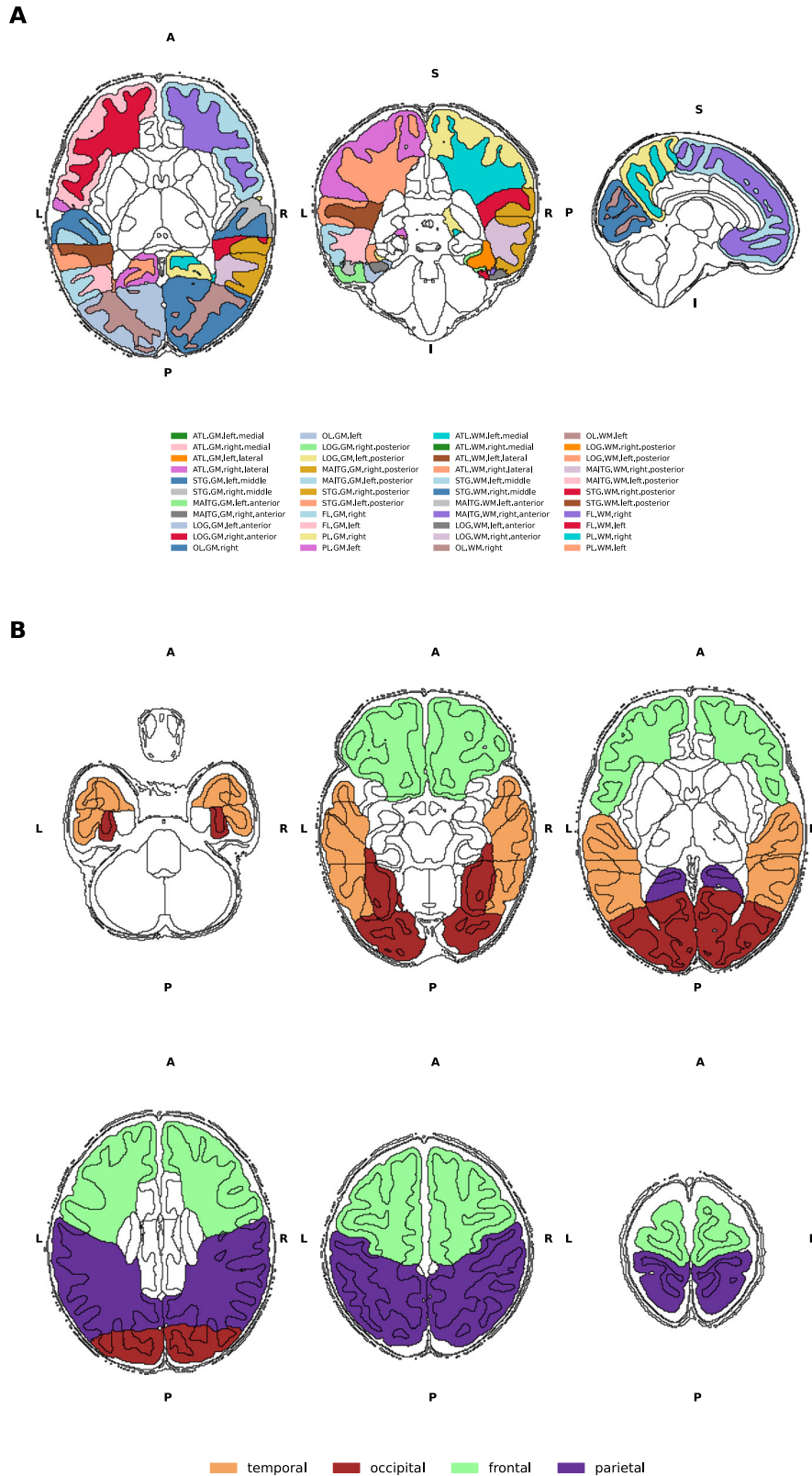


Fig. 1 Visualisation of DrawEM parcellations. **A** Visualisation of the brain regions examined in axial, coronal and sagittal views. Black outline denotes segmented brain regions. Regions found within the four cortical lobes examined in this study are coloured. **B** Six axial views from inferior to posterior indicating the boundaries of the four cortical lobes. ATL anterior temporal lobe, GPEA gyri parahippocampalis et ambiens, STG superior temporal gyrus, MAITG medial and inferior temporal gyrus, LOGGF lateral occipotemporal gyri, gyrus fusiform, CG cingulate gyrus, FL frontal lobe, PL parietal lobe, OL occipital lobe, INSU insula. WM white matter, GM grey matter. A anterior, P posterior, S superior, I inferior, L left, R right.

gene-set enrichment analysis similar to Van Scheltinga et al. [38] was carried out. For each of the 116 433 SNPs obtained from PRSice-2 after thresholding and clumping, two sets of univariate tests were performed to determine its effect on fronto-temporal and parieto-occipital lobe volumes (Volume \sim GA + PMA + TBV + Risk allele frequency + sex + ancestry PCs). The SNPs were then ranked based on their association strengths with either phenotype. Setting the cut-off threshold at p -value < 0.01 , the top-ranking SNPs were then grouped into three subsets: SNPs associated with only fronto-temporal lobe volume, SNPs associated with only parieto-occipital lobe volume, and SNPs associated with both volumes. The cut-off threshold was selected to keep the sizes of the resulting gene lists conservative [39]. To determine if elements in each SNPs subset converged on relevant biological pathways, genes containing those SNPs were probed for their functions. Here, a gene was selected if it contained the SNP of interest within its start and stop coordinates according to the human genome build 37 (<https://ctg.cncr.nl/software/magma>). Thus, for each SNPs subset, a corresponding gene list was created. Each gene list was then functionally tested against a curated database of 13 159 gene sets (pathways) obtained from MSigDB v.7.5.1 (curated canonical pathways from Reactome, KEGG, Wikipathways and Gene Ontology; <https://www.gsea-msigdb.org/gsea/msigdb/>). For each pathway, the hypergeometric test was used to determine the probability of randomly observing the set of genes in the gene list [39]. This analysis was performed using GENE2FUNC on FUMA platform [40] with 19,427 genes from the human genome Build 37 as background genes. Pathways with adjusted Bonferroni p -value $< 1.26 \times 10^{-6}$ (i.e., $0.05/(13,159 \text{ pathways} * 3 \text{ gene lists})$) and containing at least 4 overlapping genes with the gene list were considered enriched. Finally, to ensure consistency and reproducibility of the results, an additional stability test was carried out for each gene list. Here, we randomly sampled n SNPs (where n is the number of SNPs found in each SNPs subset), generated the corresponding gene list, and applied the hypergeometric method described above. This test was simulated 1000 times, and the most enriched pathway in each run was recorded. Gene sets specific to the phenotype of interest were those that were found across fewer than 5% of all random experiments.

Table 1. Demography of the European neonatal cohort included in this study.

Individuals	273
Female/Male	133/140
GA (weeks)	40.16 \pm 1.22
PMA (weeks)	41.75 \pm 1.66
Total Brain Volume (mm ³)	380,251 \pm 49,469
Birth weight (kg)	3.48 \pm 0.47

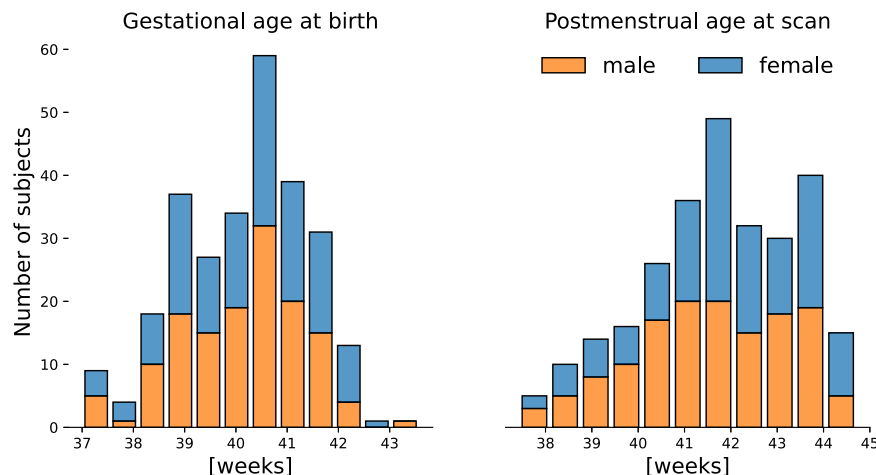


Fig. 2 Term-born European neonatal cohort. Distribution of gestational age at birth and postmenstrual age at scan of participants included in the study.

RESULTS

Higher ASD PRS associated with greater fronto-temporal volume but lower parieto-occipital volumes

We found statistically significant associations between frontal ($\beta = 0.027$, $p_{FDR} = 0.04$), parietal ($\beta = -0.037$, $p_{FDR} = 0.04$), fronto-temporal ($\beta = 0.024$, $p_{FDR} = 0.01$), and parieto-occipital lobe ($\beta = -0.033$, $p_{FDR} = 0.01$) volumes and PRS-PC1 (Fig. 3). Here, higher PRS-PC1 was associated with higher frontal and fronto-temporal volumes, but lower parietal and parieto-occipital volumes. Performing stability tests by halving or comparing the top and bottom extremes of different PRS P_T distributions showed a consistent direction of association in the reported brain regions (Supplementary Fig. 2 and Supplementary Fig. 3). Finally, consistent patterns of associations were also observed when considering all 10 PRS P_T values (Supplementary Fig. 4).

Enrichment in pathways related to neuron differentiation and synaptic membrane

From the 116 433 SNPs examined in this study, three unique SNPs subsets and their corresponding gene lists associated with fronto-temporal volume, parieto-occipital volume, or both were generated (Fig. 4A). Overrepresentation analyses of the three gene lists identified enrichment in several gene-ontology biological processes and cellular components (Supplementary Table 1). Retaining only the significant pathways found in less than 5% of times across all random simulations revealed 2 gene sets, synaptic membrane (Gene Ontology (GO) cellular component, GO: 0097060; $p = 9.5 \times 10^{-7}$) and neuron differentiation (GO biological process, GO: 0030182, $p = 7.6 \times 10^{-7}$).

DISCUSSION

We identified an association between ASD common genetic variants and regional brain lobe volumes in a cohort of term-born infants at birth. Here, we reported a positive association between fronto-temporal brain volume and ASD risk, but a negative association between parieto-occipital brain volume and ASD risk. These results show measurable differences in brain volume associated with ASD risk prior to the onset of disease. In addition, exploratory gene set enrichment analysis of the ASD common variants most associated with the examined neuroimaging phenotypes suggested possible widespread disruption to normal early development processes.

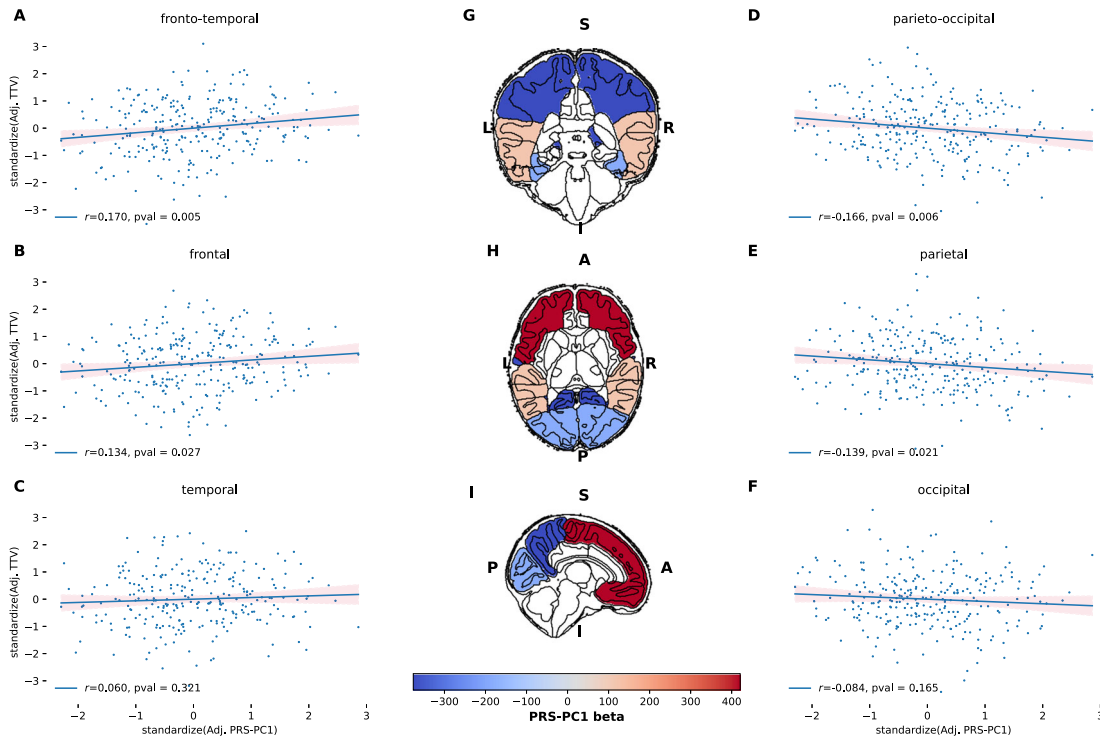


Fig. 3 Association between PRS-PC1 and regional volumes. Left **A–C** and right **D–F** panels show scatterplots denoting the correlation r and p -value between regional volumes and PRS-PC1 on the y- and x-axis respectively. Values of regional volumes and PRS-PC1 have been standardized and adjusted for GA, PMA, sex, TBV and the first 3 ancestral PCs, respectively. Middle **G–I** show brain regions overlapped with values of PRS-PC1 beta coefficient in the linear regression model, where blue and red values indicate negative and positive direction of effect; S superior, I inferior, A anterior, P posterior, L left, R right.

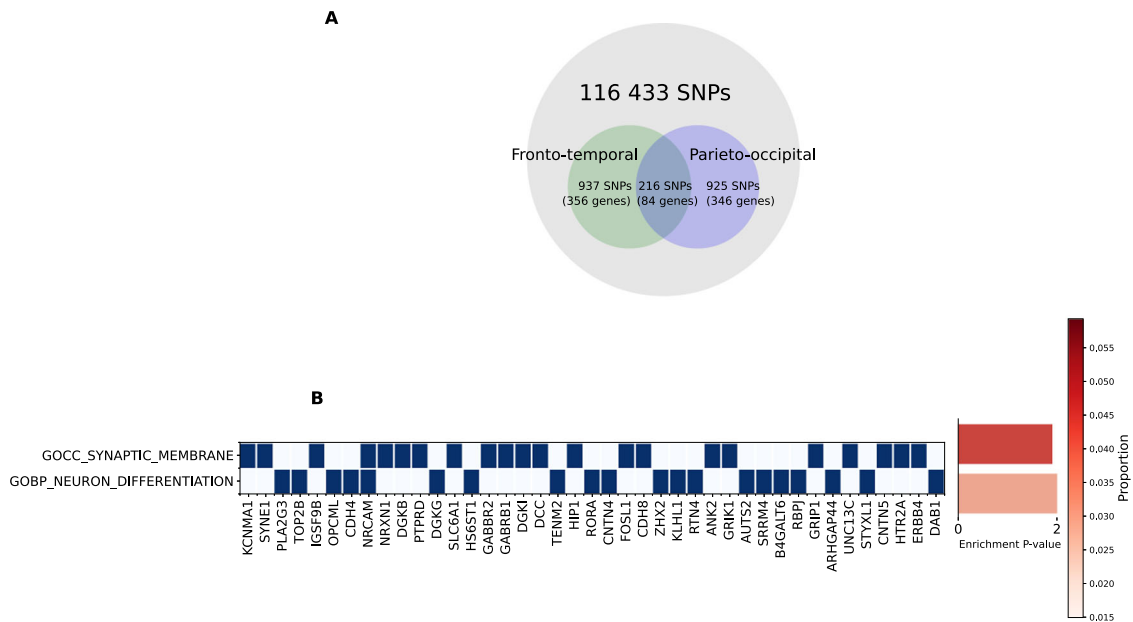


Fig. 4 Gene set-enrichment analysis. **A** Visualisation of the total SNPs examined in this study and number of SNPs and genes determined as associated with three phenotypes of interest. **B** Heatmap of genes involved in biological pathways enriched and specific (found in less than 5% across all random simulations) to the neuroimaging phenotypes of interest. Bar plot showing pathway enrichment p-value after Bonferroni correction and proportion of gene overlapped with the gene list. GOCC gene ontology cellular components, GOBP gene ontology biological pathways.

Comparison with previous examination of ASD-related structural variations

To our knowledge, this is the first study to examine the association of ASD common genetic variants with regional brain lobe volumes

in a general population at birth. Previously, in two similar but larger cohorts of children between 3–14 and 9–12 years of age, ASD PRS has been significantly associated with the cortical thickness of precentral and postcentral gyri [2] and nominally (i.e.,

did not survive multiple testing correction) associated with superior parietal gyrification [41]. Taken together, these studies suggest that ASD common genetic variants may be involved in early structural brain variations.

Evidence of abnormal cortical surface area expansion has been observed in infants with a high familial risk of ASD in the first year of life [1]. In retrospective studies of ASD children, this surface area enlargement appeared to relate to cerebral brain volume increase in ASD children between 2–4 years old [1, 13]. In both examination of cortical surface area and cerebral lobe volumes, there appeared to be regional variability associated with the disease. This study provides additional evidence for regional brain volume differences associated with ASD PRS measurable as early as birth. While it is not yet known whether such brain structural changes persist in adolescence and adulthood [42], a recent longitudinal study of ASD cases versus controls between 2 and 13 years of age found that early cerebral enlargement was maintained until middle childhood with no evidence of normalisation or regression [9].

Greater frontal and fronto-temporal volume in association with greater ASD risk is in line with existing brain imaging studies [43]. Evaluation of postmortem prefrontal cortices has suggested this may be driven by an abnormally excess number of neurons in ASD children compared with that in controls [44]. However, to our knowledge, no studies to date have identified reduced brain volume either in individuals with ASD or in association with ASD risk. While the magnitude of cerebral hyperplasia appears to vary across regions, with frontal and temporal lobes being more affected than the parietal and occipital lobes [30], our result of reduced parietal and occipital lobe volumes has not yet been reported. Given that previous exploration of ASD PRS has focused on total brain volume and global grey and white matter [3, 41], we could not draw a comparison with our current result. Interestingly, recent transcriptomic analysis of postmortem ASD brain tissues across four cortical lobes similarly found evidence of variability in the expression of risk genes along the antero-posterior axis [17]. Taken together, this suggests pathophysiology of the disease may involve disruption to the normal neuro-patterning process. Concurrently, the current study reported a consistent pattern of opposite directions of effect related to ASD common variants between fronto-temporal and parieto-occipital regions.

Clinical relevance of neuroimaging observations with pathophysiology of ASD

While the pathophysiology of ASD likely begins prenatally, the evidence suggests that subtle ASD-traits emerge during the latter part of the first and second years in high-risk infants who later develop the disease [45]. For instance, at 6 months, high-risk infants exhibit differences in gross motor and visual reception skills [46]. Interestingly, recent studies also found a significant association between ASD PRS and motor and language scores in general infant populations at 18 months [47, 48], raising the possibility of partial contributions by ASD common variants on related ASD traits. However, the current consensus is that ASD-defining features likely become pronounced only after the second year and consolidate around the fourth year, which co-occurs with the regional brain volume overgrowth [45]. Indeed, disruptions to the regions examined in this study have been implicated in reduced social and language functions and repetitive or stereotyped behaviours of ASD [49]. Nevertheless, the direction and effect of the association between regional brain lobe volumes, ASD symptoms and ASD common variants remain largely unclear and future investigation into this interplay in early life may provide important insights into the pathophysiology of the disease.

Exploratory gene set enrichment analysis

To our knowledge, there is no conventional procedure to examine the processes underpinning associations between PRS and imaging phenotypes. In this exploratory analysis, by ranking and

selecting ASD common variants that were associated with fronto-temporal and parieto-occipital volumes, we aimed to explore whether the same SNPs underlie these associations. Here, we found that while these associations were not driven by the same SNPs set, the resulting gene lists for both imaging phenotypes were enriched for neurodevelopmental processes. However, this is expected since ASD common variants are likely found in genes primarily involved in corticogenesis and with the highest expression during the prenatal period [15]. In addition, we have previously identified regional brain volume variations associated with schizophrenia PRS in the same cohort of infants [50]. Together, these preliminary results support the notion that many psychiatric disorders may have a neurodevelopmental origin and may be associated with brain structural variations before the average age of the disease diagnosis [20].

Dysregulation of multiple aspects of synaptic function and neuron development have been implicated in the disease. For instance, combinations of abnormal synaptogenesis (e.g. due to mutations in core regulators of synaptic architectures) and synaptic pruning (e.g., defects in neuronal autophagy) have been proposed to lead to increased density of dendritic spines in ASD patients [51]. Similarly, abnormalities in the control of neuronal cell differentiation may give rise to accelerated neuronal cell growth observed in ASD [52].

Limitations

The main limitation of our study is the small sample size and simplicity of PRS. Therefore, the findings presented here must be considered preliminary, and confirmation in independent samples is important. Here, only term-born infants of European ancestry were considered. This was firstly due to the known impacts of prematurity on the brain structures and secondly due to the exclusive inclusion of the Danish population in the discovery GWAS sample. In line with the latest schizophrenia GWAS [53], future inclusion of different ancestral groups in the ASD GWAS may improve the generalisability of the PRS. Finally, while overrepresentation analyses must be considered exploratory, as the analyses are biased toward larger well-studied processes [39], they may still provide relevant targets for future investigation.

CONCLUSION

In summary, our study reports positive associations between the ASD PRS with the frontal and fronto-temporal volumes, but negative with the parietal and parieto-occipital volumes in a cohort of term neonates. Whilst preliminary, the result contributes to the examination of the pathophysiology of ASD and its early emergence.

DATA AVAILABILITY

The MRI data used (dHCP third release) is freely available: <https://biomedica.github.io/dHCP-release-notes/>. The described statistical analysis can be recreated using the IPython notebook https://github.com/lehai-ml/dHCP_genetics/blob/main/notebook_results/asd/Supplementary_notebook.ipynb. Scripts used for visualising results in this study is available here: <https://github.com/lehai-ml/nimagen>.

REFERENCES

1. Hazlett HC, Gu H, Munsell BC, Kim SH, Styner M, Wolff JJ, et al. Early brain development in infants at high risk for autism spectrum disorder. *Nature*. 2017;542:348–51.
2. Khundrakpam B, Vainik U, Gong J, Al-Sharif N, Bhutani N, Kiar G, et al. Neural correlates of polygenic risk score for autism spectrum disorders in general population. *Brain Commun*. 2020;2:fcaa092. <https://doi.org/10.1093/BRAINCOMMS/FCAA092>
3. Alemamy S, Jansen PR, Muetzel RL, Marques N, El Marroun H, Jaddoe VVW, et al. Common polygenic variations for psychiatric disorders and cognition in relation

- to brain morphology in the general pediatric population. *J Am Acad Child Adolesc Psychiatry*. 2019;58:600–7.
4. Schumann CM, Bloss CS, Barnes CC, Wideman GM, Carper RA, Akshoomoff N, et al. Longitudinal magnetic resonance imaging study of cortical development through early childhood in autism. *J Neurosci*. 2010;30:4419–27.
 5. Shen MD, Nordahl CW, Li DD, Lee A, Angkustsiri K, Emerson RW, et al. Extra-axial cerebrospinal fluid in high-risk and normal-risk children with autism aged 2–4 years: a case-control study. *Lancet Psychiatry*. 2018;5:895–904.
 6. Kyriakopoulou V, Davidson A, Chew A, Gupta N, Arichi T, Nosarti C, et al. Characterisation of ASD traits among a cohort of children with isolated fetal ventriculomegaly. *Nat Commun*. 2023;14:1–10.
 7. Courchesne E, Carper R, Akshoomoff N. Evidence of brain overgrowth in the first year of life in autism. *JAMA*. 2003;290:337–44.
 8. Hazlett HC, Poe M, Gerig G, Smith RG, Provenzale J, Ross A, et al. Magnetic resonance imaging and head circumference study of brain size in autism: birth through age 2 years. *Arch Gen Psychiatry*. 2005;62:1366–76.
 9. Lee JK, Andrews DS, Ozonoff S, Solomon M, Rogers S, Amaral DG, et al. Longitudinal evaluation of cerebral growth across childhood in boys and girls with autism spectrum disorder. *Biol Psychiatry*. 2021;90:286–94.
 10. Carper RA, Courchesne E. Localized enlargement of the frontal cortex in early autism. *Biol Psychiatry*. 2005;57:126–33.
 11. Bloss CS, Courchesne E. MRI neuroanatomy in young girls with autism: a preliminary study. *J Am Acad Child Adolesc Psychiatry*. 2007;46:515–23.
 12. Kates WR, Burnette CP, Eliez S, Strunge LA, Kaplan D, Landa R, et al. Neuroanatomic variation in monozygotic twin Pairs discordant for the narrow phenotype for autism. *Am J Psychiatry*. 2004;161:539–46.
 13. Hazlett HC, Poe MD, Gerig G, Styner M, Chappell C, Smith RG, et al. Early brain overgrowth in autism associated with an increase in cortical surface area before age 2 years. *Arch Gen Psychiatry*. 2011;68:467–76.
 14. Gogtay N, Giedd JN, Lusk L, Hayashi KM, Greenstein D, Vaituzis AC, et al. Dynamic mapping of human cortical development during childhood through early adulthood. *Proc Natl Acad Sci USA*. 2004;101:8174–9.
 15. Grove J, Ripke S, Als TD, Mattheisen M, Walters RK, Won H, et al. Identification of common genetic risk variants for autism spectrum disorder. *Nat Genet*. 2019;51:431–44.
 16. Parikshak NN, Luo R, Zhang A, Won H, Lowe JK, Chandran V, et al. Integrative functional genomic analyses implicate specific molecular pathways and circuits in autism. *Cell*. 2013;155:1008.
 17. Gandal MJ, Haney JR, Wamsley B, Yap CX, Parhami S, Emani PS, et al. Broad transcriptomic dysregulation occurs across the cerebral cortex in ASD. *Nature*. 2022;611:532–9.
 18. Holland D, Chang L, Ernst TM, Curran M, Buchthal SD, Alicata D, et al. Structural growth trajectories and rates of change in the first 3 months of infant brain development. *JAMA Neurol*. 2014;71:1266–74.
 19. Knickmeyer RC, Gouttard S, Kang C, Evans D, Wilber K, Smith JK, et al. A structural MRI study of human brain development from birth to 2 years. *J Neurosci*. 2008;28:12176–82.
 20. Marín O. Developmental timing and critical windows for the treatment of psychiatric disorders. *Nat Med*. 2016;22:1229–38.
 21. Edwards AD, Rueckert D, Smith SM, Abo Seada S, Alansary A, Almalbis J, et al. The developing human connectome project neonatal data release. *Front Neurosci*. 2022;16:1–14.
 22. Cullen H, Dimitrakopoulou K, Patel H, Curtis C, Batalle D, Gale-Grant O et al. Common genetic variation important in early subcortical brain development. Preprint at <https://www.medrxiv.org/content/10.1101/2022.08.11.22278677v1> (2022).
 23. Hughes EJ, Winchman T, Padormo F, Teixeira R, Wurie J, Sharma M, et al. A dedicated neonatal brain imaging system. *Magn Reson Med*. 2017;78:794–804.
 24. Cordero-Grande L, Hughes EJ, Hutter J, Price AN, Hajnal JV. Three-dimensional motion corrected sensitivity encoding reconstruction for multi-shot multi-slice MRI: application to neonatal brain imaging. *Magn Reson Med*. 2018;79:1365–76.
 25. Kuklisova-Murgasova M, Quaghebeur G, Rutherford MA, Hajnal JV, Schnabel JA. Reconstruction of fetal brain MRI with intensity matching and complete outlier removal. *Med Image Anal*. 2012;16:1550–64.
 26. Makropoulos A, Gousias IS, Ledig C, Aljabar P, Serag A, Hajnal JV, et al. Automatic whole brain MRI segmentation of the developing neonatal brain. *IEEE Trans Med Imaging*. 2014;33:1818–31.
 27. Gousias IS, Edwards AD, Rutherford MA, Counsell SJ, Hajnal JV, Rueckert D, et al. Magnetic resonance imaging of the newborn brain: manual segmentation of labelled atlases in term-born and preterm infants. *Neuroimage*. 2012;62:1499–509.
 28. Makropoulos A, Robinson EC, Schuh A, Wright R, Fitzgibbon S, Bozek J, et al. The developing human connectome project: a minimal processing pipeline for neonatal cortical surface reconstruction. *Neuroimage*. 2018;173:88–112.
 29. Makropoulos A, Aljabar P, Wright R, Hüning B, Merchant N, Arichi T, et al. Regional growth and atlas of the developing human brain. *Neuroimage*. 2016;125:456–78.
 30. Courchesne E, Pierce K, Schumann CM, Redcay E, Buckwalter JA, Kennedy DP, et al. Mapping early brain development in autism. *Neuron*. 2007;56:399–413.
 31. Auton A, Abecasis GR, Altshuler DM, Durbin RM, Bentley DR, Chakravarti A, et al. A global reference for human genetic variation. *Nature*. 2015;526:68–74.
 32. Pedersen CB, Bybjerg-Grauholm J, Pedersen MG, Grove J, Agerbo E, Bækvad-Hansen M, et al. The iPSYCH2012 case-cohort sample: new directions for unravelling genetic and environmental architectures of severe mental disorders. *Mol Psychiatry*. 2018;23:6–14.
 33. Coombes BJ, Ploner A, Bergen SE, Biernacka JM. A principal component approach to improve association testing with polygenic risk scores. *Genet Epidemiol*. 2020;44:676–86.
 34. Bergen SE, Ploner A, Howrigan D, O'Donovan MC, Smoller JW, Sullivan PF, et al. Joint contributions of rare copy number variants and common SNPs to risk for schizophrenia. *Am J Psychiatry*. 2019;176:29–35.
 35. Alnæs D, Kaufmann T, Van Der Meer D, Córdova-Palamera A, Rokicki J, Moberget T, et al. Brain heterogeneity in schizophrenia and its association with polygenic risk. *JAMA Psychiatry*. 2019;76:739–48.
 36. Maglanoc LA, Kaufmann T, van der Meer D, Marquand AF, Wolfers T, Jonassen R, et al. Brain connectome mapping of complex human traits and their polygenic architecture using machine learning. *Biol Psychiatry*. 2020;87:717–26.
 37. Gale-Grant O, Fenn-Moltu S, França LGS, Dimitrova R, Christiaens D, Cordero-Grande L, et al. Effects of gestational age at birth on perinatal structural brain development in healthy term-born babies. *Hum Brain Mapp*. 2022;43:1577–89.
 38. Terwisscha Van Scheltinga AF, Bakker SC, Van Haren NEM, Derks EM, Buizer-Voskamp JE, Boos HBM, et al. Genetic schizophrenia risk variants jointly modulate total brain and white matter volume. *Biol Psychiatry*. 2013;73:525–31.
 39. Huang DW, Sherman BT, Lempicki RA. Systematic and integrative analysis of large gene lists using DAVID bioinformatics resources. *Nat Protoc*. 2009;4:44–57.
 40. Watanabe K, Taskesen E, van Bochoven A, Posthuma D. Functional mapping and annotation of genetic associations with FUMA. *Nat Commun*. 2017;8:1–11.
 41. Alemany S, Blok E, Jansen PR, Muetzel RL, White T. Brain morphology, autistic traits, and polygenic risk for autism: a population-based neuroimaging study. *Autism Res*. 2021;14:2085–99.
 42. Sacco R, Gabriele S, Persico AM. Head circumference and brain size in autism spectrum disorder: a systematic review and meta-analysis. *Psychiatry Res Neuroimaging*. 2015;234:239–51.
 43. Crucitti J, Hyde C, Enticott PG, Stokes MA. A systematic review of frontal lobe volume in autism spectrum disorder revealing distinct trajectories. *J Integr Neurosci*. 2022;21:57.
 44. Courchesne E, Mouton PR, Calhoun ME, Semendeferi K, Ahrens-Barbeau C, Hallet MJ, et al. Neuron number and size in prefrontal cortex of children with autism. *JAMA*. 2011;306:2001–10.
 45. Piven J, Elison JT, Zylka MJ. Toward a conceptual framework for early brain and behavior development in Autism. *Mol Psychiatry*. 2017;22:1385–94.
 46. Estes A, Zwaigenbaum L, Gu H, St. John T, Paterson S, Elison JT, et al. Behavioral, cognitive, and adaptive development in infants with autism spectrum disorder in the first 2 years of life. *J Neurodev Disord*. 2015;7:1–10.
 47. Takahashi N, Harada T, Nishimura T, Okumura A, Choi D, Iwabuchi T, et al. Association of genetic risks with autism spectrum disorder and early neurodevelopmental delays among children without intellectual disability. *JAMA Netw Open*. 2020;3:e1921644–e1921644.
 48. Serdarevic F, Tiemeier H, Jansen PR, Alemany S, Xerxa Y, Neumann A, et al. Polygenic risk scores for developmental disorders, neuromotor functioning during infancy, and autistic traits in childhood. *Biol Psychiatry*. 2020;87:132–8.
 49. Ecker C, Bookheimer SY, Murphy DGM. Neuroimaging in autism spectrum disorder: brain structure and function across the lifespan. *Lancet Neurol*. 2015;14:1121–34.
 50. Le H, Dimitrakopoulou K, Patel H, Curtis C, Cordero-Grande L, Edwards AD, et al. Effect of schizophrenia common variants on infant brain volumes: cross-sectional study in 207 term neonates in developing human connectome project. *Transl Psychiatry*. 2023;13:1–8.
 51. Zhang H. Synaptic dysregulation in autism spectrum disorders. *J Neurosci Res*. 2020;98:2111–4.
 52. Schafer ST, Paquola ACM, Stern S, Gosselin D, Ku M, Pena M, et al. Pathological priming causes developmental gene network heterochronicity in autistic subject-derived neurons. *Nat Neurosci*. 2019;22:243–55.
 53. Trubetskoy V, Pardiñas AF, Qi T, Panagiotaropoulou G, Awasthi S, Bigdeli TB, et al. Mapping genomic loci implicates genes and synaptic biology in schizophrenia. *Nature*. 2022;604:502–8.

ACKNOWLEDGEMENTS

Data were provided by the developing Human Connectome Project, KCL-Imperial-Oxford Consortium and the work was funded by ERC grant agreement no. 319456, the Wellcome EPSRC Centre for Medical Engineering at Kings College London (WT 203148/Z/16/Z) and by the National Institute for Health Research (NIHR) Biomedical Research Centre based at Guy's and St Thomas' NHS Foundation Trust and King's College London. The views expressed are those of the authors and not necessarily those of the NHS, the National Institute for Health Research or the Department of Health. The funders had no role in the design and conduct of the study; collection, management, analysis, and interpretation of the data; preparation, review, or approval of the manuscript; and decision to submit the manuscript for publication. We are grateful to the families who generously supported this trial. HL is supported by the UK Medical Research Council (MR/N013700/1) and King's College London member of the MRC Doctoral Training Partnership in Biomedical Sciences. HC is an academic clinical lecturer in Clinical Genetics at Kings College London and is supported by the NIHR. LCG received support from the Comunidad de Madrid-Spain Support for R&D Projects [BGP18/00178]. The authors acknowledge the use of the research computing facility at King's College London, Rosalind (<https://rosalind.kcl.ac.uk>).

AUTHOR CONTRIBUTIONS

HL, HC, MD, JDT designed the study and wrote the manuscript. KD, ADE, JH, LCG, HP, CC, HC, MD, JDT provided imaging and genetic data. HL, HC performed data analysis. HL, DF, HC, MD, JDT provided critical revision to the manuscript.

COMPETING INTERESTS

The authors declare no competing interests.

ADDITIONAL INFORMATION

Supplementary information The online version contains supplementary material available at <https://doi.org/10.1038/s41398-025-03253-2>.

Correspondence and requests for materials should be addressed to Hai Le.

Reprints and permission information is available at <http://www.nature.com/reprints>

Publisher's note Springer Nature remains neutral with regard to jurisdictional claims in published maps and institutional affiliations.



Open Access This article is licensed under a Creative Commons Attribution 4.0 International License, which permits use, sharing, adaptation, distribution and reproduction in any medium or format, as long as you give appropriate credit to the original author(s) and the source, provide a link to the Creative Commons licence, and indicate if changes were made. The images or other third party material in this article are included in the article's Creative Commons licence, unless indicated otherwise in a credit line to the material. If material is not included in the article's Creative Commons licence and your intended use is not permitted by statutory regulation or exceeds the permitted use, you will need to obtain permission directly from the copyright holder. To view a copy of this licence, visit <http://creativecommons.org/licenses/by/4.0/>.

© The Author(s) 2025